Earth and Planetary Science Letters 428 (2015) 267–280

Contents lists available at ScienceDirect

Earth and Planetary Science Letters

www.elsevier.com/locate/epsl

Globally enhanced mercury deposition during the end-Pliensbachian extinction and Toarcian OAE: A link to the Karoo–Ferrar Large Igneous Province

L.M.E. Percival [a,*], M.L.I. Witt [a,1], T.A. Mather [a], M. Hermoso [a], H.C. Jenkyns [a], S.P. Hesselbo [b], A.H. Al-Suwaidi [c], M.S. Storm [a], W. Xu [a], M. Ruhl [a]

[a] Department of Earth Sciences, University of Oxford, South Parks Road, Oxford, OX1 3AN, UK
[b] Camborne School of Mines, University of Exeter, Penryn Campus, Penryn, TR10 9EZ, UK
[c] Petroleum Geoscience Department, Petroleum Institute University and Research Centre, PO Box 2533, Abu Dhabi, United Arab Emirates

ARTICLE INFO

Article history:
Received 28 October 2014
Received in revised form 25 June 2015
Accepted 29 June 2015
Available online 29 July 2015
Editor: J. Lynch-Stieglitz

Keywords:
Oceanic Anoxic Event
Large Igneous Province
mercury
Toarcian
Karoo–Ferrar
Hg/TOC

ABSTRACT

The Mesozoic Era featured emplacement of a number of Large Igneous Provinces (LIPs), formed by the outpouring of millions of cubic kilometres of basaltic magma. The radiometric ages of several Mesozoic LIPs coincide with the dates of Oceanic Anoxic Events (OAEs). As a result of these coincidences, a causal link has been suggested, but never conclusively proven. This study explores the use of mercury as a possible direct link between the Karoo–Ferrar LIP and the coeval Toarcian OAE (T-OAE). Mercury is emitted to the atmosphere as a trace constituent of volcanic gas, and may be distributed globally before being deposited in sediments. Modern marine deposits show a strong linear correlation between mercury and organic-matter content. Results presented here indicate departures from such a simple linear relationship in sediments deposited during the T-OAE, and also during the Pliensbachian–Toarcian transition (an event that saw elevated benthic extinctions and carbon-cycle perturbations prior to the T-OAE). A number of depositional settings illustrate an increased mercury concentration in sediments that record one or both events, suggesting a rise in the depositional flux of this element. Complications to this relationship may arise from very organic-rich sediments potentially overprinting any Hg/TOC signal, whereas environments preserving negligible organic matter may leave no record of mercury deposition. However, the global distribution of coevally elevated Hg-rich levels suggests enhanced atmospheric mercury availability during the Early Toarcian, potentially aided by the apparent affinity of Hg for terrestrial organic matter, although the relative importance of aquatic *vs* terrestrial fixation of Hg in governing these enrichments remains uncertain. A perturbation in atmospheric Hg is most easily explained by enhanced volcanic output. It is suggested that extrusive igneous activity caused increased mercury flux to the Early Toarcian sedimentary realm, supporting the potential of this element as a proxy for ancient volcanism. This interpretation is consistent with a relationship between LIP formation and a perturbed carbon cycle during the Pliensbachian–Toarcian transition and T-OAE. The recording of these two distinct Hg excursions may also indicate that the Karoo–Ferrar LIP released volatiles in temporally distinct episodes, due either to multiple phases of magmatic emplacement or sporadic release of thermogenic gaseous products from intrusion of igneous material into volatile-rich lithologies.

1. Introduction

Large Igneous Provinces (LIPs) are seen in the geological record as immense emplacements of igneous material into either oceanic or continental crust (Coffin and Eldholm, 1994; Bryan and Ernst, 2008). Most provinces comprise on the order of 10^6 km^3 of chiefly tholeiitic basalt, the bulk of which is thought to have been emplaced within a million years (Bryan et al., 2010; Blackburn et al., 2013). Given the impact on the climate system witnessed after the large-scale basaltic eruptions in Iceland at Laki in 1783 (Thordarson and Self, 2003), and the much greater volume and inferred eruption rate of LIPs, it has been proposed that these huge outpourings of magma resulted in catastrophic climatic effects. This hypothesis is reinforced by coincidences (within dating error) between the radiometric ages

* Corresponding author. Tel.: +44 1865 272041.
E-mail address: lawrencp@earth.ox.ac.uk (L.M.E. Percival).
[1] Now at Department of Physiology, Anatomy and Genetics, Le Gros Clark Building, University of Oxford, South Parks Road, Oxford, OX1 3QX, UK.

http://dx.doi.org/10.1016/j.epsl.2015.06.064

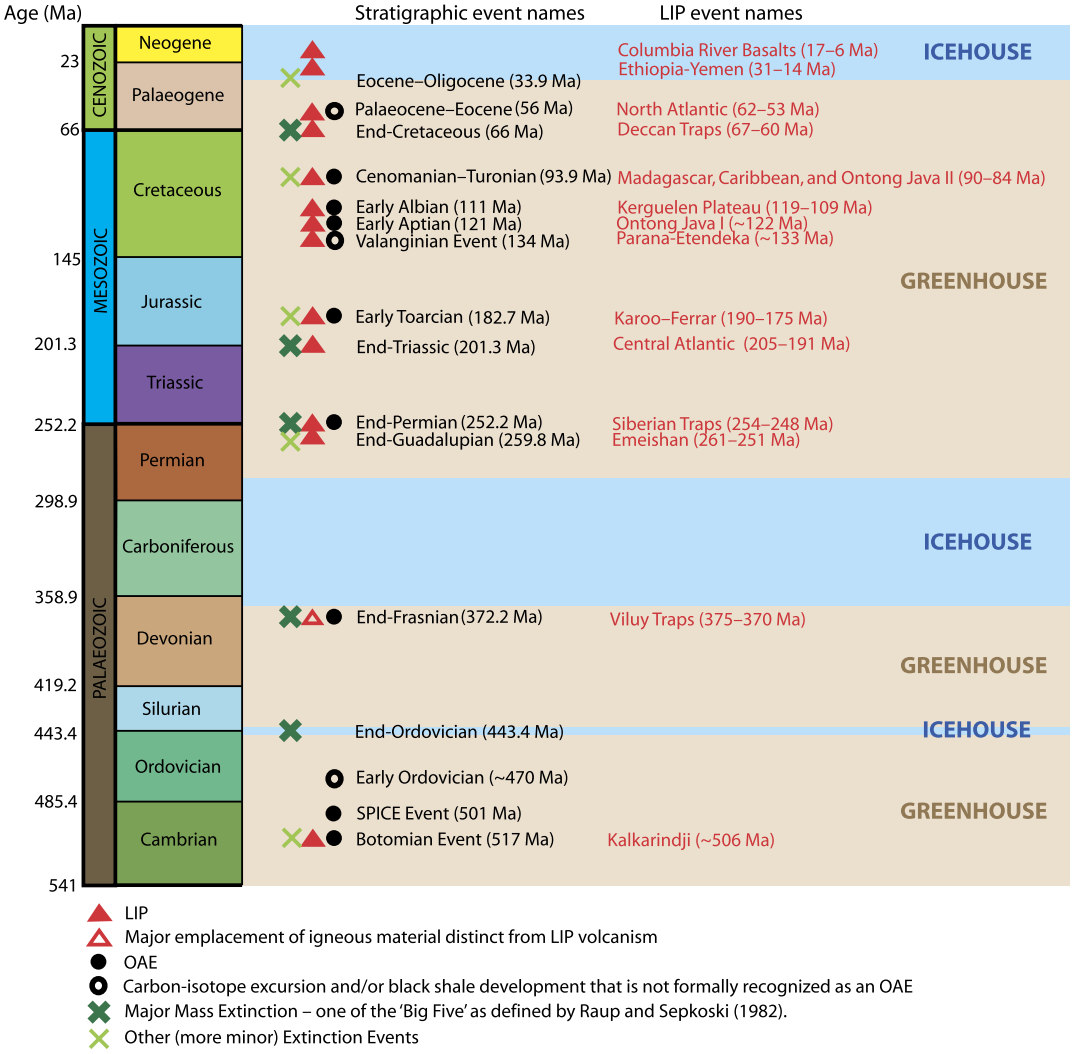

Fig. 1. An illustration of the temporal correlation of Large Igneous Provinces (LIPs) with Ocean Anoxic Events (OAEs) and/or extinction events. The correlation is best in the Mesozoic. Palaeozoic provinces are less likely to be preserved, and Cenozoic provinces were emplaced in an icehouse climate, and were consequently less likely to facilitate regional anoxia. Note gaps in the correlation include the two most recent provinces (that do not appear to have had a major environmental impact) and the end-Ordovician mass extinction (that is not associated with any known LIP). This diagram is based on the reviews of Courtillot and Renne (2003) and Wignall (2005). The dates of LIP emplacement refer to the onset of emplacement and are taken from the reviews of Courtillot and Renne (2003) and Bryan et al. (2010). The geological ages are taken from the 2014 Geological Time Scale (Geological Society of America; http://www.stratigraphy.org/ICSchart/ChronostratChart2014.pdf).

of LIPs and the dates of a number of mass extinctions and/or Oceanic Anoxic Events (OAEs) (Rampino and Strothers, 1988; Courtillot and Renne, 2003; Fig. 1).

In spite of this coincidence, there remains criticism of a simple cause-and-effect relationship between volcanism and disturbances to the global environment. The causal mechanism remains debated, usually featuring CO_2 emissions, but some quantitative estimates of LIP volatiles are not thought high enough to have significantly perturbed the carbon cycle (Caldeira and Rampino, 1990; Wignall, 2001; Self et al., 2006, 2014). In addition, the coincidence between LIP emplacement and mass extinctions is not perfect. There are LIPs whose formation does not appear to have coincided with extinctions or major environmental change (e.g. the Ethiopian and Columbia River Provinces), whilst the end-Ordovician mass extinction did not coincide with formation of a documented LIP.

One of the issues with settling this debate is that whilst the extinction/climate record is preserved in sedimentary rocks, apart from rare LIP flows and/or volcaniclastic deposits interbedded with proximal sediments, there is no well-tested uniquely volcanic tracer in sedimentary deposits, particularly for deposits situated distally from the LIP. Biostratigraphic ages of sedimentary phenomena are difficult to compare with the dates of volcanism derived from astrochronology and radiometric techniques (chiefly U–Pb), which all potentially carry attendant errors. Sampling of LIPs for dating is limited by their geographic and stratigraphic distribution, made worse by their typically poor preservation. Many oceanic LIPs may also have been partially destroyed by subduction, or broken up and obducted on to continents. A global sedimentary proxy for volcanism is a key piece of evidence to confirm the correlation between large-scale volcanism and major environmental change. A lead isotope study has linked OAE 2 (Cenomanian–Turonian boundary) to the Madagascan Province, but is the only study that uses Pb isotopes in that context, and is dependent on the assumption that silicate material can remain long enough in the atmosphere to cross hemispheres and still contribute 20–40% of silicate material to the studied sediment (Kuroda et al., 2007). Osmium and neodymium isotopes have also been used to infer volcanic output, but cannot be unambiguously distinguished from a reduction in the effects of continental weathering (Cohen et al., 2004; Zheng et al., 2013; Du Vivier et al., 2014).

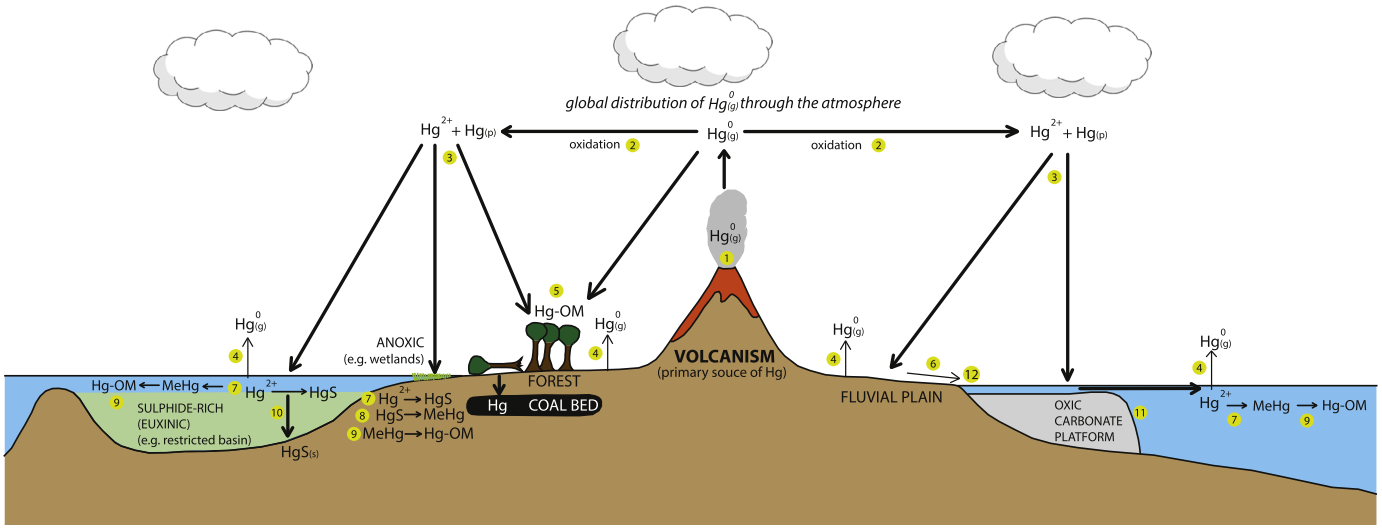

KEY:

1. Volcanic emission of primarily inert elemental mercury gas ($Hg^0_{(g)}$).
2. Oxidation of $Hg^0_{(g)}$ in the atmosphere to form particulate mercury ($Hg_{(p)}$) and soluble oxidised mercury (Hg^{2+}).
3. Deposition of atmospheric mercury as either $Hg_{(p)}$ (localized around source) or Hg^{2+} dissolved in rain (globally).
4. Biotic or abiotic reduction of Hg^{2+} to $Hg^0_{(g)}$, which is re-emitted to the atmosphere.
5. Interaction of $Hg^0_{(g)}$, $Hg_{(p)}$ and/or Hg^{2+} with forest canopy, resulting in trees adsorbing and accumulating atmospheric Hg, which may subsequently be deposited as coal and other wood-derived material.
6. Riverine flux of Hg from the terrestrial to the marine realm, mainly in mineral form or adsorbed in detrital organics.
7. In the aquatic realm, biotic or abiotic recactions on Hg^{2+} and/or reduced $Hg^0_{(g)}$ may form mercury sulphide complexes (HgS) or methylmercury (MeHg).
8. In anaerobic settings such as wetlands and lakes, sulphur-reducing bacteria absorb neutral sulphur compounds to metabolize sulphur. As a byproduct, the HgS complexes are methylated to form MeHg.
9. Bioaccumulation of lipophilic MeHg forms organo-mercury complexes (Hg-OM), although these can also form abiotically. Therefore, most aqueous Hg is scavenged and deposited to sediments by OM.
10. In sulphide-rich settings HgS becomes saturated and precipitates. Its subsequent burial removes HgS locally, inhibiting methylation.
11. In aerobic settings distal from land (where detrital OM input is minimal), Hg burial is limited by low abundance and/or burial of OM or sulphides that would scavenge aqueous Hg.
12. In coastal or fluvial settings with abundant detrital woody material, some OM will be preserved in sediments, and therefore draw-down of aqeuous Hg may occur.

Fig. 2. A simplified illustration of the natural mercury cycle, designed to highlight the large-scale features of the major pathways from volcanic emission to sedimentary deposition. An arbitrary landmass is represented that features a number of contrasting marine redox settings (anoxic wetlands, oxic carbonate platforms, and euxinic restricted basins) along its coastlines. Aquatic and atmospheric chemistry is considerably simplified here to aid clarity of illustration. The figure is primarily constructed on the basis of the reviews by Schroeder and Munthe (1998), Munthe et al. (2009) and Selin (2009), as well as the additional studies of Benoit et al. (1999) and Fleck et al. (1999).

1.1. Mercury as a tracer for distal volcanism

It is known that volcanism represents a substantial source of mercury to the atmosphere (Pyle and Mather, 2003 and references therein). Most volcanic mercury is emitted as gaseous Hg^0, which has an atmospheric residence time of 1–2 years, significantly longer than that of other volcanic metals emitted as aerosols and particles, which (depending on the size of the particle/aerosol droplet) have an atmospheric residence time on the order of weeks (Jaenicke, 1980; Schroede and Munthe, 1998; Hinkley et al., 1999; Mather et al., 2003; Bagnato et al., 2007; Witt et al., 2008). Thus, the element has a greater potential for global distribution than other volcanic trace metals, and can certainly achieve hemispheric exchange. Gaseous Hg^0 is removed from the atmosphere through oxidation by halogens, ozone, and other radicals to form reactive Hg^{2+}, which is soluble in water and typically deposited during rainfall. Particulate Hg represents a minor component of volcanic mercury, but has a much shorter residence time in the atmosphere than Hg^0, restricting it to a more localized distribution (Schroede and Munthe, 1998; Selin, 2009). In the aquatic realm, a number of biotic and abiotic processes may affect dissolved Hg^{2+}, which often result in the formation of organic–Hg complexes. Consequently, mercury is typically adsorbed onto organic matter when deposited in sediments, resulting in a roughly constant Hg/TOC ratio (TOC: Total Organic Carbon) in modern environments (Benoit et al., 2001; Outridge et al., 2007; Gehrke et al., 2009; Liu et al., 2012; Ruiz and Tomiyasu, 2015). In waters rich in sulphides, Hg-sulphide complexes may precipitate, resulting in rapid mercury burial (Benoit et al., 1999; Niessen et al., 2003). In the terrestrial realm, mercury may be deposited in soil, or taken up directly by leaves in the tree canopy (Fleck et al., 1999; Frescholtz et al., 2003; Ericksen et al., 2003), which may then result in enhanced Hg concentrations in plant tissue (Fleck et al., 1999). Fig. 2 illustrates the path from volcanism to sediment in a simplified mercury cycle.

Because volcanoes are known to expel Hg into the atmosphere, a number of studies have used the element as a tracer for historical volcanism in both ice cores and sedimentary systems (e.g. Schuster et al., 2002; Ribeiro Guevara et al., 2010). In the geological record, the first use of Hg as a proxy for volcanism was by Sanei et al. (2012), who observed a Hg excursion at the Permian–Triassic boundary in the Sverdrup Basin, Canadian Arctic, which they attributed to Hg output from the emplacement of the Siberian Traps. Moreover, when the Hg concentration observed at the end-Permian was normalized against TOC, a positive excursion in Hg/TOC ratios remained, indicating that the anomalous Hg signal was not simply derived from increased deposition of organic carbon and associated organic-Hg complexes. Comparison with the stratigraphic record of Mo/Al redox proxy suggests that the Permian–Triassic Hg/TOC anomalies do not relate to decreases in oxygenation, indicating that anoxia was not the sole cause of the anomalous Hg/TOC ratios in end-Permian sediments (Grasby et al., 2013).

Anomalous Hg concentrations have also been reported from end-Cretaceous sediments, which are attributed to the Deccan Traps (Silva et al., 2013; Sial et al., 2013, 2014). However, the reported Cretaceous Hg anomalies are not normalized against TOC, and therefore do not allow for potential lithological changes in organic-matter content governing Hg concentrations (for example, the transition between organic-poor limestone and organic-rich clay). These studies highlight the importance of considering wt% TOC alongside mercury concentrations because aquatic Hg is typically scavenged by organic matter (OM) and increased burial of such material may similarly increase Hg drawdown into sediments (Sanei et al., 2012). However, if flux and burial rate of organic

matter were great enough to overwhelm its scavenging affinity for Hg, a signal of real increased mercury input could potentially be hidden if expressed as a simple Hg/TOC ratio.

1.2. The Toarcian Oceanic Anoxic Event

The Toarcian Oceanic Anoxic Event (T-OAE) of the Early Jurassic has previously been linked to LIP volcanism (Rampino and Strothers, 1988; Duncan et al., 1997; McElwain et al., 2005; Svensen et al., 2007). The OAE was initially recognized in the marine sedimentary record by the appearance of laminated organic-rich black shale in a number of globally distributed sections, beginning at or near the top of the boreal ammonite *tenuicostatum* Zone and extending into the *falciferum* Zone above (Jenkyns, 1988). Coincident with the appearance of the black shale is a succession of carbon-isotope excursions (CIEs). Typically, an abrupt negative shift, usually about −6‰ but ranging from −3‰ to −9‰ according to material analyzed, disrupts an overarching positive excursion (Jenkyns and Clayton, 1986, 1997; Hesselbo et al., 2000; Jenkyns, 2003; Hermoso et al., 2009a). The CIEs are observed in wood, carbonate and marine organic matter at a number of locations, indicating that the carbon cycle was perturbed in both the marine and atmospheric realms. A smaller negative CIE is also observed at the Pliensbachian–Toarcian boundary, below the T-OAE level (Hesselbo et al., 2007; Littler et al., 2010).

Although negative excursions in $\delta^{13}C$ may result from a number of processes, such as a local change in organic-matter composition, the preservation of negative excursions in shallow- and deep-water carbonate, wood, and compound-specific organic matter synchronously across the globe suggests a global perturbation of the carbon cycle (Schouten et al., 2000; French et al., 2014). The most plausible explanation is that the negative excursions indicate a massive release of isotopically light carbon to the atmosphere: likely from methane clathrate release or thermogenic sources (Hesselbo et al., 2000; McElwain et al., 2005; Svensen et al., 2007). The positive excursions reflect increased burial of organic matter rich in isotopically light carbon (Jenkyns, 1988, 2010). Such disturbances to the global carbon cycle would be expected to have manifestly changed global marine and atmospheric conditions. Increased atmospheric carbon output would have raised global temperatures, potentially leading to raised sea levels, increased weathering rates, an enhanced hydrological cycle, localized eutrophic water bodies, and widespread stratified water columns (Jenkyns, 2003; Cohen et al., 2004; McArthur et al., 2008; Hermoso and Pellenard, 2014; Brazier et al., 2015). The changes to Earth's climate and sea levels would have likely resulted in elevated extinction rates. Such a rise in extinctions in marine fauna (particularly benthic groups) is observed at both the Pliensbachian–Toarcian boundary and T-OAE horizon (Little and Benton, 1995).

1.3. The Karoo–Ferrar Province

Large-scale igneous emplacements are widely distributed across South Africa (Karoo), southern South America (Chon Aike), and Droning Maud Land in Antarctica (Ferrar). The combined volume of the igneous outcrop totals more than two million cubic kilometres (Pankhurst et al., 2000), and would have been much greater in volume originally, because much of the emplaced material has been eroded or, in the case of the Ferrar, obscured by ice sheets. All of the emplacements have been radiometrically dated to the Early Jurassic by a number of techniques (i.e. Rampino and Strothers, 1988; Encarnación et al., 1996; Duncan et al., 1997; Pankhurst et al., 2000). The most recent Ar–Ar dates indicate that emplacement had commenced by 183.246 ± 0.045 Ma (Karoo) and 182.799 ± 0.033 Ma (Ferrar), and continued to 181.31 ± 0.19 Ma (Sell et al., 2014; Burgess et al., 2015). Thus emplacement occurred throughout the early- to mid-Toarcian Stage (Stage age from 2014 Geological Time Scale – Geological Society of America; http://www.stratigraphy.org/ICSchart/ChronostratChart2014.pdf). However, within individual provinces, a range of radiometric ages has been determined, which illustrate some disparity in different geographical regions (Jourdan et al., 2005). Such disparities may suggest a style of emplacement that featured multiple phases of extrusion spread over several million years, each individual phase lasting 10s–100s of millennia. This inference is supported by the interpreted emplacement styles of other LIPs, for example the Deccan Traps and Central Atlantic Magmatic Province, where individual flows show weathering surfaces and/or are separated by many metres of sediment (Widdowson et al., 1997; Marzoli et al., 2011 and references therein).

Much of the Karoo and Ferrar Provinces consist of basaltic rock, although the Ferrar Province also contains a large proportion of more silicic material (McClintock and White, 2006), and the Chon Aike emplacements are predominantly rhyolitic (Pankhurst et al., 1998). Although Hg is a trace volcanic volatile, 2×10^6 km^3 of magma would be expected to have produced a significant flux of the element. The entire emplacement may have emitted up to 150 Mt of Hg, based on previous estimates of LIP SO_2 output and Hg/SO_2 ratios at modern volcanoes (Siegel and Siegel, 1984; Thordarson and Self, 1996; Self et al., 2005, 2006; Bagnato et al., 2011, 2014; Mather et al., 2012). The significant fraction of silicic rocks in Ferrar and Chon Aike may suggest considerable explosive activity during emplacement of those provinces, increasing the potential for stratospheric injection of volatiles. Such a process would be expected to extend further the lifetime of gaseous Hg in the atmosphere, thus enhancing global distribution of the element. Furthermore, the Karoo province is thought to have intruded organic-rich shales and coals in the Karoo Basin (McElwain et al., 2005; Svensen et al., 2007). Metamorphism of organic-rich (and therefore relatively mercury-rich) lithologies may have produced thermogenic mercury gas, potentially increasing Hg output to the atmosphere still further.

1.4. Study aims

The Sanei et al. (2012) study on end-Permian mercury anomalies examined only one section thought to have been downwind of the Siberian Traps. Data from a single site do not prove global distribution of mercury simultaneous with LIP volcanism. Although the end-Cretaceous studies examined widely distributed sections, Hg concentrations were not normalized against TOC, so that an abnormal supply of this element cannot be unambiguously inferred. In this study, seven sections that record the Lower Toarcian interval are examined and analyzed for Hg concentrations at regular intervals, with Hg abundance normalized against wt% TOC. Hg abundances and Hg/TOC ratios are set against known lithology and carbon-isotope signatures of the sections to determine whether excursions in Hg/TOC coincide with volcanic events at the Pliensbachian–Toarcian boundary and/or the onset of the T-OAE. In addition, analysis of a section with variable TOC levels of Late Jurassic age – an interval not coincident with any known LIP volcanism – allows investigation of whether Hg/TOC ratios respond simply to changes in redox conditions rather than increased Hg flux due to volcanism. A further aim of this study is to establish to what extent local environmental effects may be superimposed on any global signal of volcanism.

2. Study areas

Most well-documented sedimentary records of the T-OAE are located in the northern hemisphere; the majority of them in Eu-

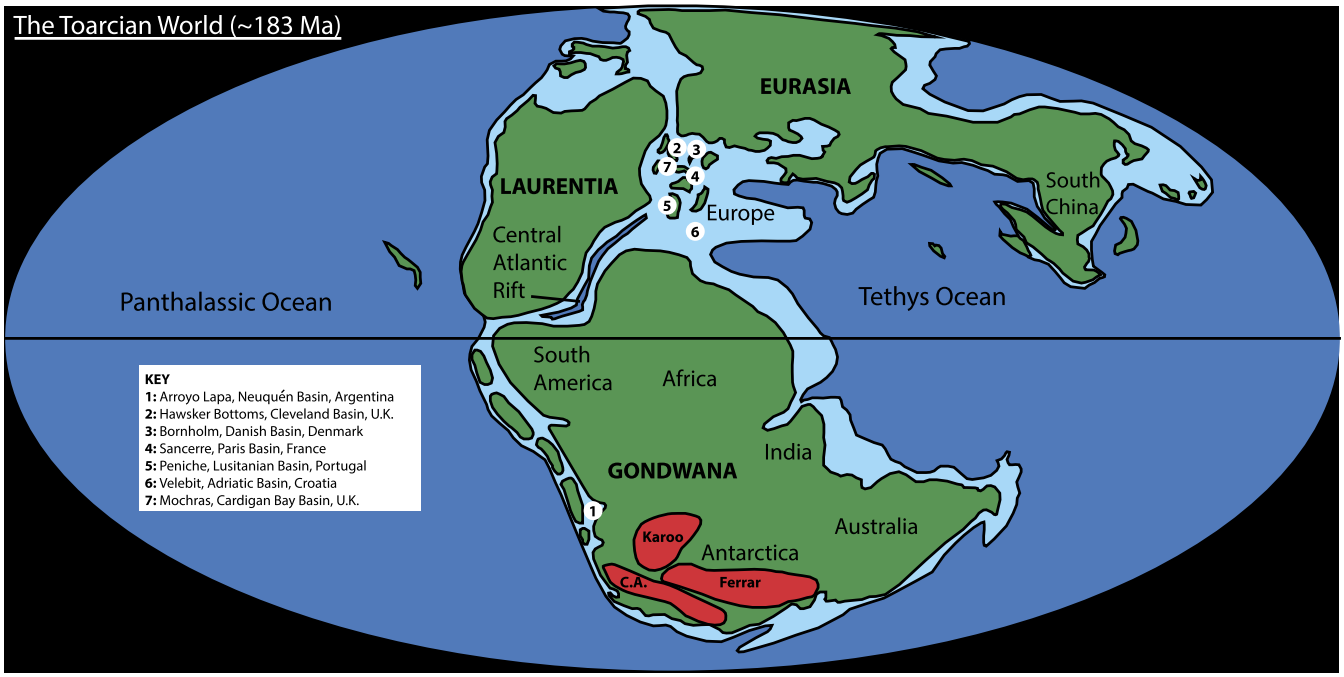

Fig. 3. A palaeogeographic reconstruction of the Early Toarcian world. The locations of the seven studied sections are indicated, as well as the Karoo–Ferrar LIP and Chon Aike (C.A.) emplacements (red; see Bryan and Ernst, 2008). Six of the sections (1, 2, 4, 5, 6, 7) are interpreted as having been deposited in a shelf marine (light blue) environment, with one section (3) deposited terrestrially (green), but none from the open oceanic realm (dark blue). The global palaeogeography is based upon Ron Blakey's Early Jurassic reconstruction (http://cpgeosystems.com/200moll.jpg). (For interpretation of the references to colour in this figure legend, the reader is referred to the web version of this article.)

rope. For this study, six European basins covering a range of facies were studied, together with the Neuquén Basin in Argentina (Fig. 3). The T-OAE horizon is recorded in all seven sections by a characteristic negative carbon-isotope excursion and/or accompanying biostratigraphy (see supplementary data). An Upper Jurassic section through the Kimmeridge Clay of the U.K. was examined as the organic-rich control from a period not associated with LIP volcanism.

2.1. Arroyo Lapa, Neuquén Basin, Argentina

As a southern hemisphere locality recording the T-OAE, the Neuquén back-arc basin contains a record relatively proximal to the Karoo–Ferrar Province. During Toarcian times, the basin would have been situated within about 1000 kilometres from extrusive centres. The lithology alternates between cross-bedded sandstone, siltstone, and black shale, and contains abundant marine fossils, particularly ammonites (Al-Suwaidi et al., 2010). Therefore, the section is interpreted as representing a marine setting on the edge of the Gondwanan supercontinent. Proximity to land is supported by the presence of macroscopic wood. The shale is locally rich in framboidal pyrite and, in one section, illustrates an increase in TOC up to a maximum of 8 wt% near the boundary between the *tenuicostatum* and *hoelderi* ammonite Zones, coincident with a stepwise decrease of 6‰ in $\delta^{13}C_{org}$ and $\delta^{13}C_{wood}$ (Al-Suwaidi et al., 2010). These indicators suggest a trend towards anoxic/euxinic conditions coincident with a perturbation in the marine and atmospheric carbon cycles.

There is evidence for local arc volcanism to the west of the Neuquén Basin in the form of volcaniclastic sedimentary grains. This local volcanism may have resulted in an enhanced background Hg/TOC ratio prior to the T-OAE at Arroyo Lapa. However, because of the greater size and eruptive rates of the Karoo–Ferrar, an excursion from the LIP should significantly exceed any local enhancement of Hg.

2.2. Hawsker Bottoms, Cleveland Basin, Yorkshire, U.K.

The Lower Toarcian strata of Yorkshire are dominated by dark grey shale, locally rich in ammonites and belemnites. In the uppermost *tenuicostatum* and overlying *falciferum* zones these sediments become black and laminated, with local carbonate concretions of centimetre to metre scale (Howarth, 1962). Coeval with the black shale is a large excursion in $\delta^{13}C$ of −7‰, developed in both bulk organic matter and fossil wood centred in the *falciferum exaratum* Subzone (Jenkyns and Clayton, 1997; Hesselbo et al., 2000; Kemp et al., 2005). Additionally, a smaller negative excursion in $\delta^{13}C_{org}$ is recorded below the T-OAE level at the Pliensbachian–Toarcian boundary (Littler et al., 2010).

Local to regional anoxia/euxinia during the T-OAE is indicated by framboidal pyrite, a sulphur-isotope excursion, increased TOC and S concentrations, organic biomarkers for green sulphur bacteria, and the millimetre laminated organic-rich nature of the shale itself (Jenkyns and Clayton, 1997 Wignall et al., 2005; McArthur et al., 2008; Gill et al., 2011; Kemp et al., 2011; French et al., 2014). The T-OAE horizon also records an excursion towards radiogenic osmium isotopes, indicative of enhanced continental weathering, possibly resulting from a more dynamic hydrological cycle during the T-OAE (Cohen et al., 2004).

2.3. Bornholm, Danish Basin, Denmark

Unlike most European basins of the Jurassic, the Danish Basin contains sediments primarily laid down in a paralic environment, ranging from fluvial to marginal marine. Consequently, the bulk of the organic matter preserved at Bornholm is terrestrial in nature, consisting predominantly of wood (Hesselbo et al., 2000). The negative excursion in the $\delta^{13}C_{wood}$ at Bornholm is therefore a good indication that a carbon-cycle perturbation affected the atmosphere as well as the marine realm (Hesselbo et al., 2000). Because Bornholm preserves a near-terrestrial environment, the ammonite biostratigraphy applied to most other Toarcian sections

cannot be utilized. However, the size and shape of the CIE preserved in the Bornholm wood is similar to those from Lower Toarcian sediments at other locations (Hesselbo et al., 2007; Hesselbo and Pieńkowski, 2011). Available palynology also indicates identification of Lower Toarcian sediments at this locality (Koppelhus and Nielsen, 1994).

2.4. Sancerre, Paris Basin, France

The Sancerre Borehole penetrated a typical north European Toarcian marine succession with abundant marl and shale whose organic-carbon content is relatively high, and the OAE itself registered by millimetre-laminated black shale. As elsewhere, the onset of the OAE is also marked by a stepwise fall of 6‰ in $\delta^{13}C_{carb}$ (Hermoso et al., 2009a, 2012). Additionally, geochemical excursions in manganese and iron are observed (Hermoso et al., 2009b). Such geochemical excursions, together with the aforementioned black shale, indicate an anoxic to euxinic water column. This interpretation is supported by an absence of benthic fauna. An additional manganese excursion is recorded at the Pliensbachian–Toarcian boundary, although there is no accompanying negative excursion in $\delta^{13}C_{carb}$ at this horizon (Hermoso et al., 2009b).

2.5. Peniche, Lusitanian Basin, Portugal

The Peniche section of the Lusitanian Basin is characterized by coccolith-bearing marls and limestones, containing ammonites and brachiopods, that record a hemipelagic environment through the Late Pliensbachian and Early Toarcian interval. The presence of macroscopic pyritized wood throughout the section indicates the former presence of landmasses proximal to the basin. Marly sediments developed during the start of the Toarcian, but black shale typical of an OAE is almost absent, and TOC levels remain low (<1%) throughout the majority of the section, suggesting that persistent anoxic conditions did not develop during the T-OAE (Hesselbo et al., 2007). However, abrupt iron, magnesium, and manganese enrichment indicates that seawater chemistry was characterized by reduced species of these metals during the Early Toarcian (Hermoso et al., 2009b). The onset of these trace-element excursions takes place at the boundary between the *polymorphum* and *levisoni* ammonite zones, and coincides with an abrupt negative excursion in $\delta^{13}C_{carb}$ of −2‰. There is also a carbon-isotope excursion at the Pliensbachian–Toarcian boundary, which coincides with elevated manganese concentrations (Hesselbo et al., 2007; Hermoso et al., 2009b). The Pliensbachian–Toarcian boundary and T-OAE horizon both record a negative excursion in $\delta^{44}Ca$, from which enhanced weathering rates during those intervals have been inferred (Brazier et al., 2015). This interpretation is consistent with the proportional increase in siliciclastics and the appearance of mass-transport deposits at the base of the *levisoni* Zone (Hesselbo et al., 2007). Such observations support the notion of an enhanced hydrological cycle and elevated weathering rates interpreted to have been present during the Early Toarcian in Europe (Cohen et al., 2004).

2.6. Velebit, Adriatic Basin, Croatia

The Velebit sections in Croatia derive from a Tethyan carbonate platform of Early Jurassic age. The Pliensbachian and lowest Toarcian sediments comprise largely lithiotid (bivalve) limestone. These sediments are succeeded in the Lower Toarcian by intensely bioturbated “spotted” limestone that is locally dolomitized (Vlahović et al., 2005). Within the spotted limestone beds an excursion of −3‰ in $\delta^{13}C$ of carbonate is recorded. There is also a clear positive excursion of 1–2‰ above the negative excursion (Sabatino et al., 2013).

As platform carbonates, the sediments represent a shallow-water oxic marine environment that retained relatively constant marine chemistry before, during, and after the T-OAE. A small increase in manganese concentration is observed coincident with the onset of the negative CIE, indicating a minor change in redox chemistry during the Early Toarcian, but there is no evidence to support the development of significantly oxygen-depleted conditions (Sabatino et al., 2013).

2.7. Mochras, Cardigan Bay Basin, U.K.

The Mochras core provides one of the most expanded records of the Early Jurassic in the world and has yielded abundant ammonites and belemnites. The core records a marine environment, likely relatively deep marine with open access to the Central Atlantic Ocean (Sellwood and Jenkyns, 1975). The inferred depositional setting of a well-mixed basin is supported by the relatively low TOC concentrations (1–2.5 wt%), which are significantly lower than those observed in the Early Jurassic Paris and Cleveland Basins that are thought to have been restricted and density-stratified (Jenkyns and Clayton, 1997; Jenkyns, 2010). Macroscopic wood is recorded in abundance throughout the section, indicating a significant terrestrial influx, which is further indicated in the upper *spinatum* Zone and *exaratum* Subzone by the appearance of centimetre-scale graded and laminated quartz-rich gravity-flow deposits, and the increased abundance of detrital material. $\delta^{13}C$ excursions are recorded in both carbonates and bulk organic matter, illustrating a positive excursion throughout the Early Toarcian stage, but with an abrupt negative excursion in the *exaratum* Subzone of the *falciferum* Zone (Jenkyns and Clayton, 1997; Jenkyns, 2003). A convincing negative excursion in $\delta^{13}C$ has not yet been reported from the Pliensbachian–Toarcian boundary in the Mochras core.

2.8. The Kimmeridge Clay (control section)

The facies of the Kimmeridge Clay are similar to those recorded in Early Toarcian basins, but instead formed during the Kimmeridgian and Tithonian stages of the Late Jurassic. No known LIP (or local volcanism) dates to that time. If volcanism were the major cause of sedimentary Hg/TOC anomalies then they should be absent from the Kimmeridge Clay. Therefore analysis of an interval within the Kimmeridge Clay was carried out to test whether Hg/TOC excursions can be produced merely through changes in marine redox chemistry (Hg is redox-sensitive), or as a result of varying lithological or environmental processes/conditions.

The shale is organic-rich (TOC can exceed 30%), and biomarkers for green sulphur bacteria and pyrite framboids are locally present, indicating prolonged anoxic–euxinic conditions in the water column (Tyson et al., 1979; Tribovillard et al., 1994; van Kaam-Peters et al., 1998; Morgans-Bell et al., 2001; van Dongen et al., 2006).

3. Methods

For each basin, sections were analyzed from a few metres below the Pliensbachian–Toarcian boundary to a few metres above the base of the negative CIE. Sample resolution was variable, ranging from every 10 cm to every 50 cm (see supplementary data). Two analyses were carried out: (1) analysis for mercury content, (2) analysis for TOC wt% content and type (based on other organic carbon analyses, e.g. Hydrogen Indices) if no pre-existing data were available.

3.1. Analysis for mercury

Mercury analysis was conducted using the RA-915 Portable Mercury Analyzer with PYRO-915 Pyrolyzer, Lumex (as described

by Bin et al., 2001). 50 ± 2 mg of powdered sample was weighed into a glass measuring boat and its precise mass determined. The sample was then placed into the pyrolyzer (set at Mode 1), which heated it to 700 °C. This process volatilized the mercury in the sample, with the resulting gas analysed spectrally to detect and calculate the Hg concentration. As a standard, five 50 ± 2 mg samples of peat (NIMT/UOE/FM/001 – Inorganic Elements in Peat) with a known mercury concentration of 169 ± 7 ng/g were analyzed prior to processing of each sample-set and, throughout analysis, a sample of peat was analyzed after approximately every tenth sample. Fifteen peat-standard samples, of varying masses between 10 and 90 mg, were also used to calibrate the Lumex.

3.2. Analysis of total organic carbon

TOC analyses were conducted using the Rock Eval 6, and carried out only on samples where there were no pre-existing TOC data. Approximately 20 mg of each sample were measured into gauze crucibles and their precise mass determined. A carousel was loaded with up to twenty-four crucibles, five of which would contain the standard IFP 160000.

During analysis the samples spent 25 minutes in a pyrolysis furnace, which fed nitrogen gas through the sample at 650 °C, removing lower molecular weight compounds with no oxidation. The sample then spent 45 minutes in an oxidation oven, which fed purified air through the sample at 850 °C to decompose organic matter. The resultant CO and CO_2 were analyzed spectrally to give the TOC percentage of the sample. The full method is described by Espitalié et al. (1977). This analysis also determined the ratio of hydrogen and oxygen to carbon in the sample, from which the Hydrogen and Oxygen Indices (HI and OI) were calculated. Additionally, T_{max} (temperature at which maximum cracking of kerogen in a sample occurs), and total inorganic carbon were derived from this method. Hydrogen Indices are of particular interest, as in immature, non-oxidized organic matter they can be used to infer organic matter type. Generally, low HI (<100 mgHC/gTOC – HC: hydrocarbons) is indicative of woody/terrestrial organic matter, whilst much higher HI (500–600 mgHC/gTOC) is indicative of marine planktonic organic matter (Tissot and Welte, 1984).

4. Results

4.1. Rock-Eval data

The Hg and TOC results are presented in Fig. 4 (for the Kimmeridge Clay) and Fig. 5 (for all Toarcian sections). For other Rock-Eval data such as Hydrogen and Oxygen Indices, Total Inorganic Carbon and T_{max}, see supplementary data. The results from the Rock Eval show that wt% TOC is very high (>10 wt%) at both Hawsker Bottoms and Sancerre at the T-OAE horizon (see also Jenkyns and Clayton, 1997). Such high preservation of organic matter likely results from the development of stratified euxinic watermasses at both locations during that time (Jenkyns, 2010 and references therein). By contrast, Peniche, Arroyo Lapa, Bornholm and Mochras all record far lower TOC percentages (<2%), and negligible organic matter is preserved in the limestone beds at Velebit.

Hydrogen Indices data were collected for five sections (Hawsker Bottoms, Arroyo Lapa, Bornholm, Sancerre, and Peniche), and indicates that Sancerre and Hawsker Bottoms have high values (400–600 mgHC/gTOC), whereas Peniche, Bornholm and Arroyo Lapa have rather lower ones (<200 mgHC/gTOC). Peniche, Bornholm and Arroyo Lapa also contain abundant macroscopic woody material in the analyzed sections, and the presence of dominantly terrestrial organic matter is supported by such low HI values. Although other processes may affect HI, such as thermal maturation or degradation of marine organic matter, other Rock Eval data (e.g. Oxygen Indices and T_{max}) suggest that this is not the case here, and that the HI values do result from the dominance of wood in the bulk organic matter (see supplementary data).

4.2. Hg concentrations and Hg/TOC ratios

Hawsker Bottoms, Peniche, and Mochras all record an abrupt and short-lived positive excursion in Hg concentrations and Hg/TOC ratios coincident with the Pliensbachian–Toarcian Boundary. Arroyo Lapa also records a similar abrupt and short-lived positive excursion in Hg/TOC, but significantly below the putative Pliensbachian–Toarcian boundary. This apparent mismatch may result from incomplete, incorrect or different biostratigraphy compared to Europe. Bornholm, Peniche, Arroyo Lapa and Mochras all record abrupt positive excursions in Hg concentrations and Hg/TOC ratios coincident with the onset of the negative carbon-isotope excursion during the T-OAE. Sancerre and Hawsker Bottoms record similar excursions in Hg concentrations, but no rise in Hg/TOC ratios, a phenomenon that may result from overprinting of any signal by the anomalously high TOC concentrations at the T-OAE level at these locations. This interpretation is supported by the absence of a linear relationship between Hg/TOC at the T-OAE horizon: Hg concentrations rise, but TOC concentrations proportionally rise further. Moreover, at Sancerre and Hawsker Bottoms Hg concentrations reach 200–300 ppb. This degree of enrichment is substantially higher than that observed in modern sediments with similar organic-carbon content and higher than the Hg concentrations recorded in the organic-rich Kimmeridge Clay samples, suggesting that Hg fluxes were higher than normal in these north European localities during the Pliensbachian–Toarcian transition and T-OAE, despite there being no resultant increase in Hg/TOC ratios for the latter event. In the Kimmeridge Clay, Hg and TOC values oscillate, but do so in tandem, resulting in a linear relationship between Hg and TOC. Such a relationship is similar to that observed at a number of modern locations, where Hg/TOC ratios are low and relatively consistent, between 0.01 and 0.02 (Gerkhe et al., 2009; Liu et al., 2012; Ruiz and Tomiyasu, 2015).

Very low Hg concentrations are present in the Velebit limestones. However, negligible TOC or sulphides are preserved in these sediments (see Section 2.6; note also the absence of TOC data in Fig. 5F), and as these are the two geochemical species that draw down mercury to sediments, their absence may explain the paucity of Hg.

5. Discussion

5.1. Possible local causes of Hg perturbations

The discovery of Lower Toarcian anomalies in Hg concentrations and Hg/TOC ratios in both Argentina and across Europe suggests that they result from a global trigger rather than local perturbations. However, because the Pliensbachian–Toarcian boundary and T-OAE are commonly associated with changes in lithological and sedimentation rate, such phenomena need to be considered as possible drivers of Hg perturbations

If it is assumed that atmospheric mercury concentrations are constant and Hg is deposited in sedimentary environments at a constant rate, then a reduction in sedimentation rate would result in increased Hg concentrations in bulk rock. However, to achieve the perturbations observed in the Early Toarcian would require a five to tenfold reduction in sedimentation rate across many basins at the same time, which is highly unlikely. In addition, an excursion towards radiogenic Sr-isotopes has shown that a major decrease in sedimentation rate did occur abruptly at Hawsker Bottoms during the T-OAE, whilst this was not the case during the Pliensbachian–Toarcian transition (McArthur et al., 2000). In con-

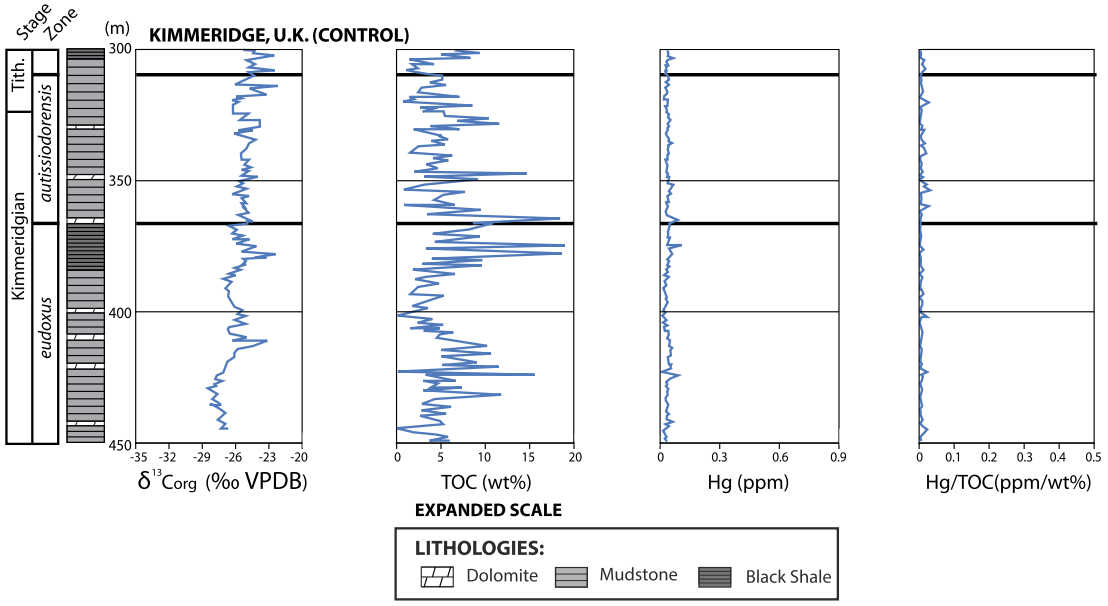

Fig. 4. $\delta^{13}C$, Total Organic Carbon (TOC), Hg and Hg/TOC data from sections from the Kimmeridge Clay (used as a control). The blue lines represent raw data. Biostratigraphic horizons are represented by bold black horizontal lines. Hg measurements have up to ±10% uncertainty; TOC measurements up to ±2% uncertainty, resulting in a net uncertainty of approximately ±10.2% for Hg/TOC measurements. Stratigraphic heights are in metres, Stage refers to the Stage in geological time; Zone refers to biostratigraphic ammonite Zones that subdivide that stage. Tith. indicates Tithonian. The simplified lithology, TOC data and carbon-isotope data are sourced from Morgans-Bell et al. (2001). (For interpretation of the references to colour in this figure legend, the reader is referred to the web version of this article.)

trast, there is a Hg anomaly at the Pliensbachian–Toarcian boundary at Hawsker Bottoms, but not at the T-OAE horizon, the opposite of what should occur if the perturbations were controlled by sedimentation rate.

That a change in lithology might have caused mercury anomalies is discounted on the basis that changes in sediment type are observed in the studied section of the Kimmeridge Clay without any shift in Hg/TOC ratios. In addition, large Hg anomalies are observed during the Toarcian at Mochras, where the lithology remains relatively constant. Although both the Pliensbachian–Toarcian boundary and T-OAE level at Mochras coincide with sediments containing increased detrital material, mercury influx to the marine realm in such a context typically takes place through bonding of Hg onto surfaces of detrital organic matter (see Section 1.1). Therefore, an increase in sedimentary Hg through detrital influx would not be expected to change Hg/TOC ratios significantly. Clearly, the Hg/TOC ratios do increase at both the Pliensbachian–Toarcian boundary and the T-OAE horizon (Fig. 5). The results from Mochras support the conclusion from the Kimmeridge Clay that lithological changes do not result in significant changes in Hg/TOC.

It could be argued that the change in marine redox chemistry during the T-OAE may aid concentration of Hg in sediments. If the spread of anoxic conditions during the T-OAE were the cause of the mercury anomalies, then it would be expected that Hg/TOC ratios in the Kimmeridge Clay (which also records anoxic/euxinic conditions) should also be high. However, Hg/TOC ratios are low in the Kimmeridge Clay, equivalent to modern background levels and pre-T-OAE background levels (Liu et al., 2012). The absence of an excursion in Hg/TOC ratios in the Kimmeridge Clay suggests that anoxic conditions do not concentrate Hg independently of concentrating organic matter. Such an inference is supported by other data. For example, a linear Hg/TOC correlation was retained in Mediterranean sapropels deposited under both oxic and anoxic depositional conditions during the mid-Pleistocene (Gerkhe et al., 2009). Similarly, Grasby et al. (2013) showed that the variations in Hg/TOC ratios do not correlate with variations in redox proxies in the Permian–Triassic sediments of the Sverdrup Basin. Both studies, as well as the results from the Kimmeridge Clay in this paper, indicate that redox changes are not the major control on sedimentary Hg/TOC ratios.

Hence, redox chemistry, lithological changes, sedimentation rate are all discounted as major factors responsible for the Hg concentration and Hg/TOC ratio excursions observed in Lower Toarcian sediments. An external, global, trigger is a more plausible explanation than local influences. However, local conditions may still influence Hg records: in environments with very high production and preservation of organic carbon any Hg/TOC perturbation may be overprinted (such as the stratified basins preserved at Hawsker Bottoms and Sancerre), whilst negligible burial of organic carbon may eliminate any possibility of recording a potential Hg perturbation, even under conditions of increased flux of the element into

Fig. 5. $\delta^{13}C$, Total Organic Carbon (TOC), Hg and Hg/TOC data from sections from Arroyo Lapa (A), Hawsker Bottoms (B), Bornholm (C), Sancerre (D), Peniche (E), Velebit F) and Mochras (G). The blue lines represent raw data. All stratigraphic heights are in metres, Stage refers to the Stage in geological time; Zone refers to biostratigraphic ammonite Zones that subdivide that stage (except at Bornholm where miospore and dinoflagellate Zones are used). *tenui.* and Pliens. indicate *tenuicostatum* Zone and Pliensbachian Stage, respectively. Biostratigraphic horizons are represented by bold black horizontal lines, with dashed lines representing an area where the precise location of a biostratigraphic boundary is uncertain. The vertical black bar and dark grey shading indicate the stratigraphic range of the T-OAE, as indicated by the positive and negative excursions in $\delta^{13}C$. Hg measurements have up to ±10% uncertainty; TOC measurements have up to ±2% uncertainty, resulting in a net uncertainty of approximately ±10.2% for Hg/TOC measurements. Velebit (F) lacks TOC data as the TOC content at that section is negligible. Carbon-isotope data are sourced as follows: Arroyo Lapa from Al-Suwaidi et al. (2010); Hawsker Bottoms from Kemp et al. (2011) and Littler et al. (2010); Bornholm from Hesselbo et al. (2000); Sancerre from Hermoso et al. (2009a); Peniche from Hesselbo et al. (2007); Velebit from Sabatino et al. (2013); Mochras from Jenkyns and Clayton (1997). TOC data are either determined in this study, or sourced as follows: Arroyo Lapa from Al-Suwaidi et al. (2010) and new data; Hawsker Bottoms from Littler et al. (2010) and Jenkyns and Clayton (1997). The lithological columns shown are representative and simplified. For more detailed lithological columns see the following references: Al-Suwaidi et al. (2010) for Arroyo Lapa; Littler et al. (2010) for Hawsker Bottoms; Hesselbo et al. (2000) for Bornholm; Hermoso et al. (2009a) for Sancerre; Hesselbo et al. (2007) for Peniche; Vlahovic et al. (2005) for Velebit; O'Sullivan et al. (1972) for Mochras. (For interpretation of the references to colour in this figure legend, the reader is referred to the web version of this article.)

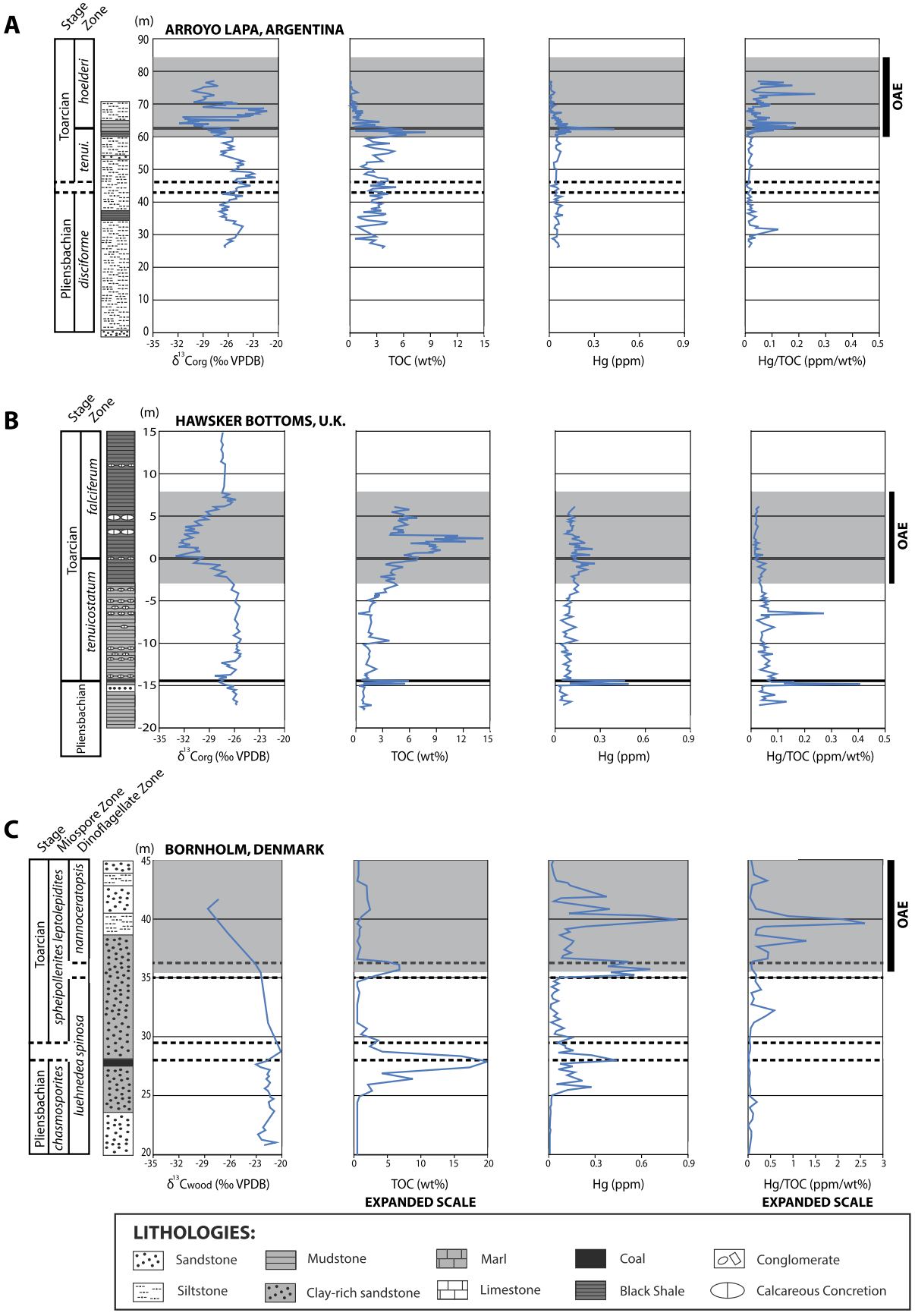

Fig. 5. (*Continued*)

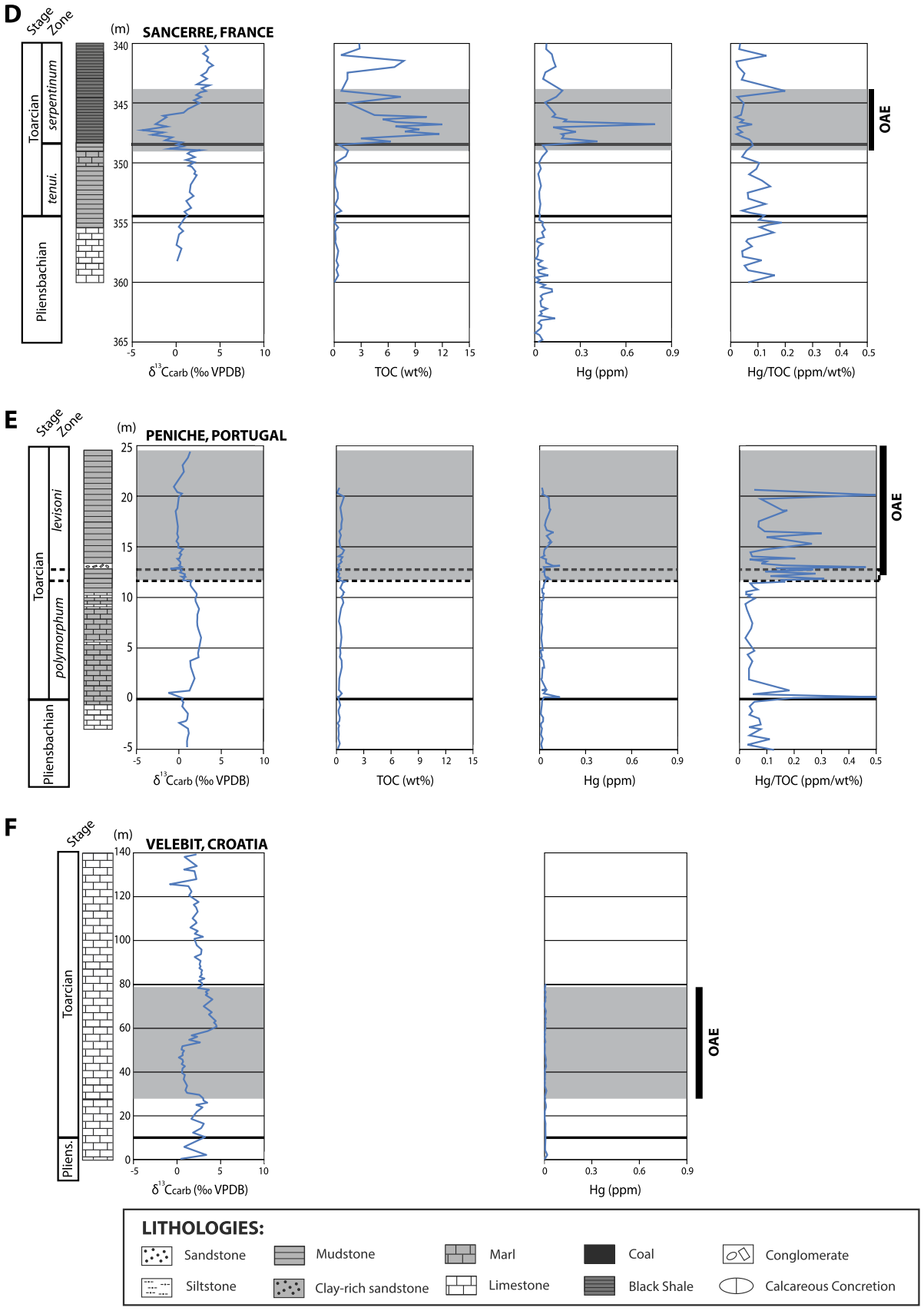

Fig. 5. (*Continued*)

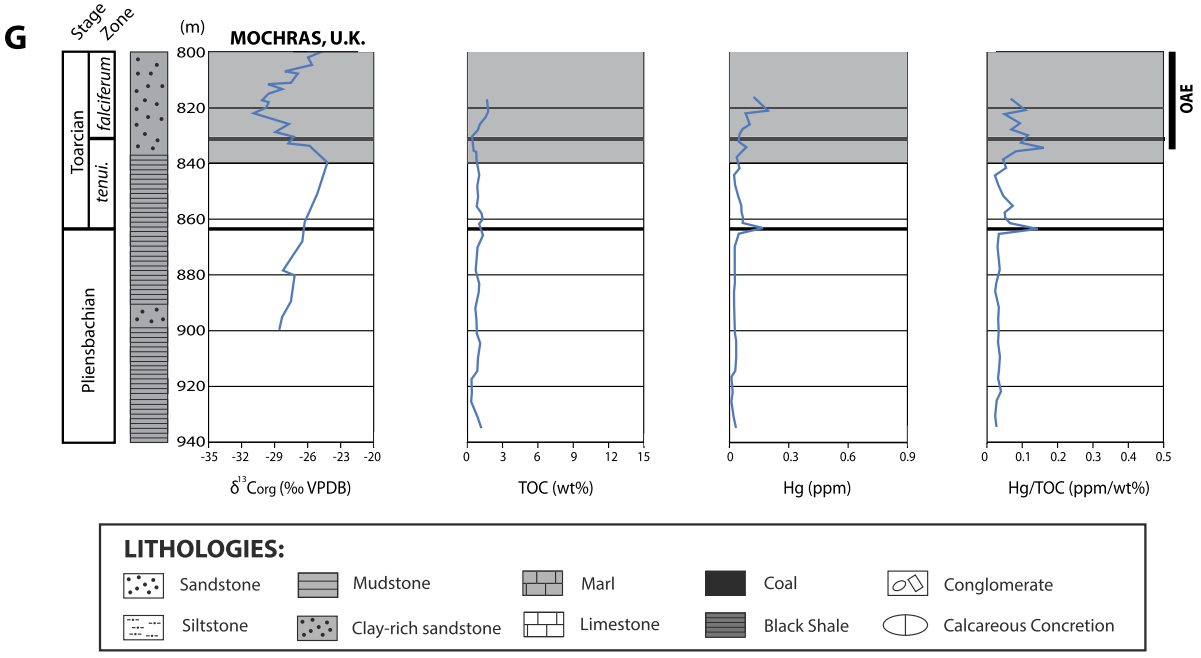

Fig. 5. (*Continued*)

the sedimentary environment (such as the carbonate-platform environment preserved at Velebit).

5.2. Volcanism as a cause of global Hg perturbations

Elevated concentrations of sedimentary mercury are observed on a global scale in Toarcian sediments. In the modern world, global transport of mercury is predominantly achieved atmospherically (Schroeder and Munthe, 1998) and there is no reason to assume that this was not also the case during the Jurassic Period. The data therefore suggest that atmospheric mercury concentrations were enhanced during the Early Toarcian. This inference is supported by the predominance of terrestrial OM in sections where Hg excursions are recorded (Mochras, Peniche, Arroyo Lapa and Bornholm). If levels of atmospheric mercury were enhanced, then it would be expected that any vegetation canopy would adsorb more Hg, particularly increasing its concentration in terrestrial organic matter (Frescholtz et al., 2003). However, there is still a possibility that such relative enrichment might have been subsequently overprinted by aquatic Hg-organic chemistry once the terrestrial OM entered the water column. Therefore, the prevalence of Hg/TOC excursions in sections with abundant woody material does not in itself signify an atmospheric perturbation in Hg. However, it is suggestive of this possibility, particularly given that the global distribution of Hg excursions also suggests elevated levels of atmospheric Hg during the Early Toarcian.

In the natural world, large-scale output of mercury to the atmosphere would be most easily achieved by widespread wildfires, large-scale volcanism, or release of thermogenic Hg (related to volcanism or a bolide impact). There is no evidence for widespread wildfires or bolide impact in the Toarcian, so the simplest explanation for globally enhanced mercury during the Toarcian is major volcanic activity, or release of thermogenic Hg following interaction between magma and country rock during large-scale igneous activity. The Karoo, Ferrar, and Chon Aike Provinces would have provided a large-scale volcanic source for enhanced atmospheric mercury during the Early–Mid Toarcian, the approximate age of the three provinces determined by radiometric dating, and the Karoo is known to have intruded organic-rich shales and coals, potentially producing additional, thermogenic, Hg output (see Section 1.3).

A key result of this work is that if perturbations in sedimentary Hg do indeed result from large-scale volcanism, there was not only LIP volcanism coincident with the T-OAE, as proposed by numerous studies, but also a precursor phase of LIP volcanism coincident with the Pliensbachian–Toarcian boundary. This supposition is best illustrated by the data from Peniche, Arroyo Lapa and Mochras, with absence of one or both Lower Toarcian Hg/TOC excursions at other sections possibly resulting from conditions local to those palaeogeographies, as discussed above. Two episodes of LIP emplacement separated by a significant period of time is suggestive of a multiple-phase emplacement of the Karoo–Ferrar–Chon Aike complex. Such a pattern is consistent with the notion that the three provinces formed separately from the same superplume, and therefore may have been emplaced at slightly different times (Pankhurst et al., 2000; Burgess et al., 2015). Moreover, individual LIPs are apparently emplaced as a series of large-scale magmatic pulses separated by quiescent periods lasting tens or hundreds of millennia (Blackburn et al., 2013; Self et al., 2014 and references therein). The multiple excursions observed in Hg/TOC (particularly at Mochras, Arroyo Lapa and Peniche) may reflect this style of magmatic emplacement. Alternatively, it is possible that magmatic activity of the three provinces took place throughout the Early Toarcian, and the mercury perturbations only occurred during magmatic interaction with organic-rich shales or coals, allowing release of thermogenic Hg. Such a possibility is compatible with the coincidence in timing of the Hg perturbations with the negative carbon-isotope excursions, which have been related by some authors to release of thermogenic carbon from metamorphism of coal or organic-rich shales (McElwain et al., 2005; Svensen et al., 2007).

6. Conclusions

This study has expanded on previous work (e.g., Sanei et al., 2012) by using Hg concentrations and Hg/TOC ratios as a global-scale proxy for LIP volcanism in the geological record. The main aim was to identify a relationship between the Karoo–Ferrar–Chon Aike Provinces and Early Toarcian climate perturbations, whilst also aiming to ascertain whether local effects could mask any

global excursion. Evidence for the influence of localized conditions on the Hg excursion record is observed at Hawsker Bottoms, Sancerre, and Velebit. If there is no organic-matter burial, then Hg burial will also be negligible and no excursion can be recorded (Velebit). Conversely, if organic matter burial is so great as to outweigh the effects of organo-Hg scavenging, any potential excursion in Hg/TOC will be overprinted by excess TOC deposition (Hawsker Bottoms and Sancerre). Consequently, palaeogeography and depositional environment must be carefully considered when evaluating Hg concentrations observed in the geological record.

In spite of the local environment issues outlined above, globally distributed positive excursions in both absolute Hg concentrations and Hg/TOC ratios of Lower Toarcian sediments are observed in this study, particularly at Peniche, Arroyo Lapa, Mochras and Bornholm. These excursions are coincident with the well-known negative carbon-isotope excursions associated with the Pliensbachian–Toarcian boundary and Toarcian Oceanic Anoxic Event. Due to the presence of the Toarcian Hg/TOC excursions in sedimentary rocks from Argentina and across Europe, and the documented global transportation of mercury in the modern atmosphere, it is here proposed that the positive excursions in sedimentary mercury reflect enhanced atmospheric Hg concentrations, an enhancement most likely derived from increased output of volcanic Hg from three LIPs of Early Jurassic age. Thus, the geochemical signatures illustrated here can be related specifically to the emplacement of the coeval Karoo–Ferrar–Chon Aike LIP. The record of enhanced atmospheric Hg during both the end-Pliensbachian extinction and T–OAE seen in some sections may support a multi-phase emplacement of the Karoo–Ferrar–Chon Aike complexes, diachronous emplacement of individual provinces, or a sporadic release of thermogenic volatiles.

Acknowledgements

We gratefully acknowledge Nadia Sabatino and Igor Vlahović for supply of samples from Velebit, Croatia, and Alberto Riccardi, Susana Damborenea and Miguel Manceñido for help in collecting and dating material from Arroyo Lapa, Argentina. We would also like to thank the two anonymous reviewers for their feedback, which has been invaluable in the revision of this paper. We acknowledge NERC (NE/G01700X/1) and the Leverhulme Trust for funding.

Appendix A. Supplementary material

Supplementary material related to this article can be found online at http://dx.doi.org/10.1016/j.epsl.2015.06.064.

References

Al-Suwaidi, A.H., Angelozzi, G.N., Baudin, F., Damborenea, S.E., Hesselbo, S.P., Jenkyns, H.C., Mancenido, M.O., Riccardi, A.C., 2010. First record of the Early Toarcian Oceanic Anoxic Event from the Southern Hemisphere, Neuquén Basin, Argentina. J. Geol. Soc. 167, 633–636. http://dx.doi.org/10.1144/0016-76492010-025.

Bagnato, E., Aiuppa, A., Parello, F., Calabrese, S., D'Alessandro, W., Mather, T.A., McGonigle, A.J.S., Pyle, D.M., Wängberg, I., 2007. Degassing of gaseous (elemental and reactive) and particulate mercury from Mount Etna volcano (Southern Italy). Atmos. Environ. 41, 7377–7388. http://dx.doi.org/10.1016/j.atmosenv.2007.05.060.

Bagnato, E., Aiuppa, A., Parello, F., Allard, P., Shinohara, H., Liuzzo, F., Giudice, G., 2011. New clues on the contribution of Earth's volcanism to the global mercury cycle. Bull. Volcanol. 73, 497–510. http://dx.doi.org/10.1007/s00445-010-0419-y.

Bagnato, E., Tamburello, G., Avard, G., Martinez-Cruz, M., Enrico, M., Fu, X., Sprovieri, M., Sonke, J.E., 2014. Mercury fluxes from volcanic and geothermal sources: an update. Special Publications, vol. 410. Geological Society, London.

Benoit, J.M., Gilmour, C.C., Mason, R.P., Heyes, R., 1999. Sulfide controls on mercury speciation and bioavailability to methylating bacteria in sediment pore waters. Environ. Sci. Technol. 33, 951–957. http://dx.doi.org/10.1021/es9808200.

Benoit, J.M., Mason, R.P., Gilmour, C.C., Aiken, G.R., 2001. Constants for mercury binding by dissolved organic matter isolates from the Florida Everglades. Geochim. Cosmochim. Acta 65, 4445–4451. http://dx.doi.org/10.1016/S0016-7037(01)00742-6.

Bin, C., Xiaoru, W., Lee, F.S.C., 2001. Pyrolysis coupled with atomic absorption spectrometry for the determination of mercury in Chinese medical materials. Anal. Chim. Acta 447, 161–169.

Blackburn, T.J., Olsen, P.E., Bowring, S.A., McLean, N.M., Kent, D.V., Puffer, J., McHone, G., Troy Rasbury, E., Et-Touhami, M., 2013. Zircon U–Pb geochronology links the End-Triassic extinction with the Central Atlantic magmatic province. Sci. Express 1234204. http://dx.doi.org/10.1126/science.1234204.

Brazier, J., Suan, G., Tacail, T., Simon, L., Martin, J.E., Mattioli, E., Balter, V., 2015. Calcium isotope evidence for dramatic increase of continental weathering during the Toarcian oceanic anoxic event (Early Jurassic). Earth Planet. Sci. Lett. 411, 164–176. http://dx.doi.org/10.1016/j.epsl.2014.11.028.

Bryan, S.E., Ernst, R.E., 2008. Revised definition of Large Igneous Provinces (LIPs). Earth-Sci. Rev. 86, 175–202. http://dx.doi.org/10.1016/j.earscirev.2007.08.008.

Bryan, S.E., Peate, I.U., Peate, D.W., Self, S., Jerram, D.A., Mawby, M.R., Marsh, J.S., Miller, J.A., 2010. The largest volcanic eruptions on Earth. Earth-Sci. Rev. 102, 207–229. http://dx.doi.org/10.1016/j.earscirev.2010.07.001.

Burgess, S.D., Bowring, S.A., Fleming, T.H., Elliot, D.H., 2015. High-precision geochronology links the Ferrar large igneous province with early-Jurassic ocean anoxia and biotic crisis. Earth Planet. Sci. Lett. 415, 90–99. http://dx.doi.org/10.1016/j.epsl.2015.01.037.

Caldeira, K., Rampino, M., 1990. Deccan volcanism, greenhouse warming, and the Cretaceous/Tertiary boundary. Spec. Pap., Geol. Soc. Am. 247, 117–124. http://dx.doi.org/10.1130/SPE247-p117.

Coffin, M.F., Eldholm, O., 1994. Large igneous provinces: crustal structure, dimensions, and external consequences. Rev. Geophys. 32 (1), 1–36.

Cohen, A.S., Coe, A.L., Harding, S.M., Schwark, L., 2004. Osmium isotope evidence for the regulation of atmospheric CO_2 by continental weathering. Geology 32, 157–160. http://dx.doi.org/10.1130/G20158.1.

Courtillot, V., Renne, P.R., 2003. On the ages of flood basalt events. C. R. Géosci. 335, 113–140. http://dx.doi.org/10.1016/S1631-0713(03)00006-3.

Du Vivier, A.D.C., Selby, D., Sageman, B.B., Jarvis, I., Gröcke, D.R., Voigt, S., 2014. Marine $^{187}Os/^{188}Os$ isotope stratigraphy reveals the interaction of volcanism and ocean circulation during Oceanic Anoxic Event 2. Earth Planet. Sci. Lett. 389, 23–33. http://dx.doi.org/10.1016/j.epsl.2013.12.024.

Duncan, R.A., Hooper, P.R., Rehacek, J., Marsh, J.S., Duncan, A.R., 1997. The timing and duration of the Karoo igneous event, southern Gondwana. J. Geophys. Res. 102, 18127–18138.

Encarnación, J.P., Fleming, T.H., Elliot, D.H., Eales, H.V., 1996. Synchronous emplacement of Ferrar and Karoo dolerites and the early break-up of Gondwana. Geology 24, 535–538.

Ericksen, J.A., Gustin, M.S., Schorran, D.E., Johnson, D.W., Lindberg, S.E., Coleman, J.S., 2003. Accumulation of atmospheric mercury in forest foliage. Atmos. Environ. 37, 1613–1622. http://dx.doi.org/10.1016/S1352-2310(03)00008-6.

Espitalié, J., Madec, M., Tissot, B., Menning, J.J., Leplat, P., 1977. Source rock characterization methods for petroleum exploration. In: Procedures of the 1977 Offshore Technology Conference, vol. 3, pp. 439–443.

Fleck, J.A., Grigal, D.F., Nater, E.A., 1999. Mercury uptake by trees: an observational experiment. Water Air Soil Pollut. 115, 513–523.

French, K.L., Sepúlveda, J., Trabucho-Alexandre, J., Gröcke, D.R., Summons, R.E., 2014. Organic geochemistry of the early Toarcian oceanic anoxic event in Hawsker Bottoms, Yorkshire, England. Earth Planet. Sci. Lett. 390, 116–127. http://dx.doi.org/10.1016/j.epsl.2013.12.033.

Frescholtz, T.F., Gustin, M.S., Schorran, D.E., Fernandez, G.C.J., 2003. Assessing the source of mercury in foliar tissue of quaking aspen. Environ. Toxicol. Chem. 22, 2114–2119. http://dx.doi.org/10.1002/etc.5620220922.

Gehrke, G.E., Blum, J.D., Meyers, P.A., 2009. The geochemical behaviour and isotopic composition of Hg in a mid-Pleistocene western Mediterranean sapropel. Geochim. Cosmochim. Acta 73, 1651–1665. http://dx.doi.org/10.1016/j.gca.2008.12.012.

Gill, B.C., Lyons, T.W., Jenkyns, H.C., 2011. A global perturbation to the sulfur cycle during the Toarcian Oceanic Anoxic Event. Earth Planet. Sci. Lett. 312, 484–496. http://dx.doi.org/10.1016/j.epsl.2011.10.030.

Grasby, S.E., Sanei, H., Beauchamp, B., Chen, Z., 2013. Mercury deposition through the Permo-Triassic Biotic Crisis. Chem. Geol. 351, 209–216. http://dx.doi.org/10.1016/j.chemgeo.2013.05.022.

Hermoso, M., Le Callonec, L., Minoletti, F., Renard, M., Hesselbo, S.P., 2009a. Expression of the Early Toarcian negative carbon-isotope excursion in separated carbonate microfractions (Jurassic, Paris Basin). Earth Planet. Sci. Lett. 277, 194–203. http://dx.doi.org/10.1016/j.epsl.2008.10.013.

Hermoso, M., Minoletti, F., Le Callonnec, L., Jenkyns, H.C., Hesselbo, S.P., Rickaby, R.E.M., Renard, M., de Rafélis, M., Emmanuel, L., 2009b. Global and local forcing of Early Toarcian seawater chemistry: a comparative study of different paleoceanographic settings (Paris and Lusitanian basins). Paleoceanography 24, PA4208. http://dx.doi.org/10.1029/2009PA001764.

Hermoso, M., Minoletti, F., Rickaby, R.E.M., Hesselbo, S.P., Baudin, F., Jenkyns, H.C., 2012. Dynamics of a stepped carbon-isotope excursion: ultra high-resolution

study of Early Toarcian environmental change. Earth Planet. Sci. Lett. 319, 45–54. http://dx.doi.org/10.1016/j.epsl.2011.12.021.

Hermoso, M., Pellenard, P., 2014. Continental weathering and climatic changes inferred from clay mineralogy and paired carbon isotopes across the early to middle Toarcian in the Paris Basin. Palaeogeogr. Palaeoclimatol. Palaeoecol. 399, 385–393. http://dx.doi.org/10.1016/j.palaeo.2014.02.007.

Hesselbo, S.P., Pieńkowski, G., 2011. Stepwise atmospheric carbon-isotope excursion during the Toarcian Oceanic Anoxic Event (Early Jurassic, Polish Basin). Earth Planet. Sci. Lett. 301, 365–372. http://dx.doi.org/10.1016/j.epsl.2010.11.021.

Hesselbo, S.P., Gröcke, D.R., Jenkyns, H.C., Bjerrum, C.J., Farrimond, P.L., Morgans-Bell, H.S., Green, O., 2000. Massive dissociation of gas hydrate during a Jurassic Oceanic Anoxic Event. Nature 406, 392–395. http://dx.doi.org/10.1038/35019044.

Hesselbo, S.P., Jenkyns, H.C., Duarte, L.V., Oliveira, L.C.V., 2007. Carbon-isotope record of the Early Jurassic (Toarcian) Oceanic Anoxic Event from fossil wood and marine carbonate (Lusitanian Basin, Portugal). Earth Planet. Sci. Lett. 253, 455–470. http://dx.doi.org/10.1016/j.epsl.2006.11.009.

Hinkley, T.K., Lamothe, P.J., Wilson, S.A., Finnegan, D.L., Gerlach, T.M., 1999. Metal emissions from Kilauea, and a suggested revision of the estimated worldwide metal output by quiescent degassing of volcanoes. Earth Planet. Sci. Lett. 170, 315–325.

Howarth, M.K., 1962. The Jet Rock Series and Alum Shale Series of the Yorkshire coast. Proc. Yorks. Geol. Soc. 33, 381–422.

Jaenicke, R., 1980. Atmospheric aerosols and global climate. J. Aerosol Sci. 11, 577–588.

Jenkyns, H.C., 1988. The early Toarcian (Jurassic) anoxic event: stratigraphic, sedimentary, and geochemical evidence. Am. J. Sci. 288, 101–151.

Jenkyns, H.C., 2003. Evidence for rapid climate change in the Mesozoic–Paleogene greenhouse world. Philos. Trans. R. Soc., Ser. A 361, 1885–1916. http://dx.doi.org/10.1098/rsta.2003.1240.

Jenkyns, H.C., 2010. Geochemistry of Oceanic Anoxic Events. Geochem. Geophys. Geosyst. 11. http://dx.doi.org/10.1029/2009GC002788.

Jenkyns, H.C., Clayton, C.J., 1986. Black shales and carbon isotopes in pelagic sediments from the Tethyan Lower Jurassic. Sedimentology 33, 87–106.

Jenkyns, H.C., Clayton, C.J., 1997. Lower Jurassic epicontinental carbonates and mudstones from England and Wales: chemostratigraphic signals and the early Toarcian anoxic event. Sedimentology 44, 687–706. http://dx.doi.org/10.1046/j.1365-3091.1997.d01-43.x.

Jourdan, F., Feraud, G., Bertrand, H., Kampunzu, A.B., Tshoso Watkeys, M.K., Le Gall, B., 2005. Karoo large igneous province: brevity, origin, and relation to mass extinction questioned by new $^{40}Ar/^{39}Ar$ age data. Geology 33, 745–748. http://dx.doi.org/10.1130/G21632.1.

Kemp, D.B., Coe, A.L., Cohen, A.S., Schwark, L., 2005. Astronomical pacing of methane release in the Early Jurassic period. Nature 437, 396–399. http://dx.doi.org/10.1038/nature04037.

Kemp, D.B., Coe, A.L., Cohen, A.S., Weedon, G.P., 2011. Astronomical forcing and chronology of the early Toarcian (Early Jurassic) oceanic anoxic event in Yorkshire, UK. Paleoceanography 26, PA4210. http://dx.doi.org/10.1029/2011PA002122.

Koppelhus, E.B., Nielsen, L.H., 1994. Palynostratigraphy and palaeoenvironments of the lower to middle Jurassic Bagå Formation of Bornholm, Denmark. Palynology 18, 139–194.

Kuroda, J., Ogawa, N.O., Tanimizu, M., Coffin, M.F., Tokuyama, H., Kitazato, H., Ohkouchi, N., 2007. Contemporaneous massive subaerial volcanism and late cretaceous Oceanic Anoxic Event 2. Earth Planet. Sci. Lett. 256, 211–213. http://dx.doi.org/10.1016/j.epsl.2007.01.027.

Little, C.T.S., Benton, M.J., 1995. Early Jurassic mass extinction: a global-event. Geology 23, 495–498. http://dx.doi.org/10.1130/0091-7613(1995)023<0495:EJMEAG>2.3.CO;2.

Littler, K., Hesselbo, S.P., Jenkyns, H.C., 2010. A carbon-isotope perturbation at the Pliensbachian–Toarcian boundary: evidence from the Lias Group, NE England. Geol. Mag. 147, 181–192. http://dx.doi.org/10.1017/S0016756809990458.

Liu, X., Xu, L., Chen, Q., Sun, L., Wand, Y., Yan, H., Liu, Y., Luo, Y., Huang, J., 2012. Historical change of mercury pollution in remote Yongle archipelago, South China Sea. Chemosphere 87, 549–556. http://dx.doi.org/10.1016/j.chemosphere.2011.12.065.

Marzoli, A., Jourdan, F., Puffer, J.H., Cuppone, T., Tanner, L.H., Weems, R.E., Bertrand, H., Cirilli, S., Bellieni, G., De Min, A., 2011. Timing and duration of the Central Atlantic magmatic province in the Newark and Culpeper basins, eastern U.S.A. Lithos 122, 175–188. http://dx.doi.org/10.1016/j.lithos.2010.12.013.

Mather, T.A., Pyle, D.M., Oppenheimer, C., 2003. Tropospheric volcanic aerosol. In: Robock, A., Oppenheimer, C. (Eds.), Volcanism and the Earth's Atmosphere. In: Geophys. Monogr. Ser., vol. 139. AGU, Washington, DC, pp. 189–212.

Mather, T.A., Witt, M.L.I., Pyle, D.M., Quayle, B.M., Aiuppa, A., Bagnato, E., Martin, R.S., Sims, K.W.W., Edmonds, M., Sutton, A.J., Ilyinskaya, E., 2012. Halogens and trace metal emissions from the ongoing 2008 summit eruption of Kīlauea volcano, Hawai`i. Geochim. Cosmochim. Acta 83, 292–323. http://dx.doi.org/10.1016/j.gca.2011.11.029.

McArthur, J.M., Donovan, D.T., Thirwall, M.F., Fouke, B.W., Mattey, D., 2000. Strontium isotope profile of the early Toarcian (Jurassic) oceanic anoxic event, the duration of ammonite biozones, and belemnite palaeotemperatures. Earth Planet. Sci. Lett. 179, 269–285.

McArthur, J.M., Algeo, T.J., van de Schootbrugge, B., Li, Q., Howarth, R.J., 2008. Basinal restriction, black shales, Re–Os dating, and the Early Toarcian (Jurassic) oceanic anoxic event. Paleoceanography 23, PA4217. http://dx.doi.org/10.1029/2008PA001607.

McClintock, M., White, J.D.L., 2006. Large phreatomagmatic vent complex at Coombs Hills, Antarctica: wet, explosive initiation of flood basalt volcanism in the Ferrar–Karoo LIP. Bull. Volcanol. 68, 215–239. http://dx.doi.org/10.1007/s00445-005-0001-1.

McElwain, J.C., Wade-Murphy, J., Hesselbo, S.P., 2005. Changes in carbon dioxide during an oceanic anoxic event linked to intrusion into Gondwana coals. Nature 435, 479–482. http://dx.doi.org/10.1038/nature03618.

Morgans-Bell, H.S., Coe, A.L., Hesselbo, S.P., Jenkyns, H.C., Weedon, G.P., Marshall, J.E.A., Tyson, R.V., Williams, C.J., 2001. Integrated stratigraphy of the Kimmeridge Clay Formation (Upper Jurassic) based on exposures and boreholes in south Dorset, UK. Geol. Mag. 138 (5), 511–539. http://dx.doi.org/10.1017/S0016756801005738.

Munthe, J., Wängberg, I., Shang, L., 2009. The origin and fate of mercury species in the natural environment. Eur. Chlor. Sci. Doss. 14.

Niessen, S., Foucher, D., Clarisse, O., Fischer, J.C., Mikac, N., Kwokal, Z., Fajon, V., Horvat, M., 2003. Influence of sulphur cycle on mercury methylation in estuarine sediment (Seine estuary, France). J. Phys. IV 107, 953–956. http://dx.doi.org/10.1051/jp:20030456.

Outridge, P.M., Sanei, H., Stern, G.A., Hamilton, P.B., Goodarzi, F., 2007. Evidence for control of mercury accumulation rates in Canadian High Arctic lake sediments by variations of aquatic primary productivity. Environ. Sci. Technol. 41, 5259–5265. http://dx.doi.org/10.1021/es070408x.

O'Sullivan, K.N., Ivimey-Cook, H.C., Lewis, B.J., Harrison, R.K., 1972. Log of the Llanbedr (Mochras Farm) Borehole. In: Woodland, A.W. (Ed.), The Llanbedr (Mochras Farm) Borehole. In: Report of the Institute of Geological Sciences, vol. 71, pp. 11–35.

Pankhurst, R.J., Leat, P.T., Suroga, P., Rapela, C.W., Márquez, M., Storey, B.C., Riley, T.R., 1998. The Chon-Aike silicic igneous province of Patagonia and related rocks in Antarctica: a silicic large igneous province. J. Volcanol. Geotherm. Res. 81, 113–136.

Pankhurst, R.J., Riley, T.R., Fanning, C.M., Kelley, S.P., 2000. Episodic silicic volcanism in Patagonia and the Antarctic Peninsula: chronology of magmatism associated with the break-up of Gondwana. J. Petrol. 41, 605–625. http://dx.doi.org/10.1093/petrology/41.5.605.

Pyle, D.M., Mather, T.A., 2003. The importance of volcanic emissions for the global atmospheric mercury cycle. Atmos. Environ. 37, 5115–5124. http://dx.doi.org/10.1016/j.atmosenv.2003.07.011.

Rampino, M.R., Strothers, R.B., 1988. Flood basalt volcanism during the past 250 million years. Science 241, 663–668. http://dx.doi.org/10.1126/science.241.4866.663.

Raup, D.M., Sepkoski, J.J., 1982. Mass extinction in the marine fossil record. Science 215, 1501–1503.

Ribeiro Guevara, S., Meili, M., Rizzo, A., Daga, R., Arribére, M., 2010. Sediment records of highly variable mercury inputs to mountain lakes in Patagonia during the past millennium. Atmos. Chem. Phys. 10, 3443–3453. http://dx.doi.org/10.5194/acp-10-3443-2010.

Ruiz, W.L.G., Tomiyasu, T., 2015. Distribution of mercury in sediments from Kagoshima Bay, Japan, and its relationship with physical and chemical factors. Environ. Earth Sci. 74, 1175–1188. http://dx.doi.org/10.1007/s12665-015-4104-5.

Sabatino, N., Vlahović, I., Jenkyns, H.C., Scopelliti, G., Rodolfo, N., Prtoljan, B., Velić, I., 2013. Carbon-isotope record and palaeoenvironmental changes during the early Toarcian oceanic anoxic event in shallow-marine carbonates of the Adriatic Carbonate Platform in Croatia. Geol. Mag. 150, 1085–1102. http://dx.doi/org/10.1017/S0016756813000083.

Sanei, H., Grasby, S., Beauchamp, B., 2012. Latest Permian mercury anomalies. Geology 40, 63–66. http://dx.doi.org/10.1130/G32596.1.

Schouten, S., van Kaam-Peters, H.M.E., Rijpstra, W.I.C., Schoell, M., Sinninghe Damste, J.S., 2000. Effects of an oceanic anoxic event on the stable carbon isotopic composition of early Toarcian carbon. Am. J. Sci. 300, 1–22. http://dx.doi.org/10.2475/ajs.300.1.1.

Schroeder, W.H., Munthe, J., 1998. Atmospheric mercury – an overview. Atmos. Environ. 32, 809–822.

Schuster, P.F., Krabbenhoft, D.P., Naftz, D.L., Cecil, L.D., Olson, M.L., Dewild, J.F., Susong, D.D., Green, J.R., Abbott, M.L., 2002. Atmospheric mercury deposition during the last 270 years: a glacial ice core record of natural and anthropogenic sources. Environ. Sci. Technol. 36, 2303–2310. http://dx.doi.org/10.1021/es0157503.

Self, S., Thordarson, T., Widdowson, M., 2005. Gas fluxes from flood basalt eruptions. Elements 1, 283–287. http://dx.doi.org/10.2113/gselements.1.5.283.

Self, S., Widdowson, M., Thordarson, T., Jay, A.E., 2006. Volatile fluxes during flood basalt eruptions and potential effects on the global environment: a Deccan perspective. Earth Planet. Sci. Lett. 248, 518–532. http://dx.doi.org/10.1016/j.epsl.2006.05.041.

Self, S., Schmidt, A., Mather, T.A., 2014. Emplacement characteristics, time scales, and volatile release rates of continental flood basalt eruptions on Earth. In:

Keller, G., Kerr, A. (Eds.), Volcanism, Impacts and Mass Extinctions: Causes and Effects. Geological Society of America Special. Paper 505.

Selin, N.E., 2009. Global biogeochemical cycling of mercury: a review. Annu. Rev. Environ. Resour. 34, 43–63. http://dx.doi.org/10.1146/annurev.environ.051308.084314.

Sell, B., Ovtcharova, M., Guex, J., Bartolini, A., Jourdan, F., Spangenberg, J.E., Vicente, J., Schaltegger, U., 2014. Evaluating the temporal link between the Karoo LIP and climatic–biologic events of the Toarcian Stage with high-precision U–Pb geochronology. Earth Planet. Sci. Lett. 408, 48–56. http://dx.doi.org/10.1016/j.epsl.2014.10.008.

Sellwood, B.W., Jenkyns, H.C., 1975. Basins and swells and the evolution of an epeiric sea (Pliensbachian–Bajocian of Great Britain). J. Geol. Soc. 131, 373–388.

Sial, A.N., Lacerda, L.D., Ferreira, V.P., Frei, R., Marquillas, R.A., Barbosa, J.A., Gaucher, C., Windmöller, C.C., Pereira, N.S., 2013. Mercury as a proxy for volcanic activity during extreme environmental turnover: the Cretaceous–Paleogene transition. Palaeogeogr. Palaeoclimatol. Palaeoecol. 387, 153–164. http://dx.doi.org/10.1016/j.palaeo.2013.07.019.

Sial, A.N., Chen, J., Lacerda, L.D., Peralta, S., Gaucher, C., Frei, R., Cirilli, S., Ferreira, V.P., Marquillas, R.A., Barbosa, J.A., Pereira, N.S., Belmino, I.K.C., 2014. High-resolution Hg chemostratigraphy: a contribution to the distinction of chemical fingerprints of the Deccan volcanism and Cretaceous–Paleogene Boundary impact event. Palaeogeogr. Palaeoclimatol. Palaeoecol. 414, 98–115. http://dx.doi.org/10.1016/j.palaeo.2014.08.013.

Siegel, S.M., Siegel, B.Z., 1984. First estimate of annual mercury flux at the Kilauea main vent. Nature 309, 146–147.

Silva, M.V.N., Sial, A.N., Barbosa, J.A., Ferreira, V.P., Neumann, V.H., Lacerda, L.D., 2013. Carbon isotopes, rare-earth elements and mercury geochemistry across the K-T transition of the Paraíba Basin, northeastern Brazil. In: Bojar, V., Melinte-Dobrinescu, M.C., Smit, J. (Eds.), Isotopic Studies in Cretaceous Research. In: Special Publications, vol. 382. Geological Society, London, pp. 85–104. http://dx.doi.org/10.1144/SP382.2.

Svensen, H., Planke, S., Chevallier, L., Malthe-Sørenssen, A., Corfu, F., Jamtveit, B., 2007. Hydrothermal venting of greenhouse gases triggering Early Jurassic global warming. Earth Planet. Sci. Lett. 256, 554–566. http://dx.doi.org/10.1016/j.epsl.2007.02.013.

Thordarson, T., Self, S., 1996. Sulphur, chlorine and fluorine degassing and atmospheric loading by the Roza eruption, Columbia River Basalt group, Washington, USA. J. Volcanol. Geotherm. Res. 74, 49–73.

Thordarson, T., Self, S., 2003. Atmospheric and environmental effects of the 1783–1784 Laki eruption. A review and reassessment. J. Geophys. Res. 108. http://dx.doi.org/10.1029/2001JD002042.

Tissot, B.P., Welte, D.H., 1984. Petroleum Formation and Occurrence, 2nd ed. Springer-Verlag, Berlin. 699 pp.

Tribovillard, N., Desprairies, A., Lallier-Vergés, E., Betrand, P., Moureau, N., Ramdani, A., Ramanampisoa, L., 1994. Geochemical study of organic-matter rich cycles from the Kimmeridge Clay Formation of Yorkshire (UK): productivity vs anoxia. Palaeogeogr. Palaeoclimatol. Palaeoecol. 108, 165–181. http://dx.doi.org/10.1016/0031-0182(94)90028-0.

Tyson, R.V., Wilson, R.C.L., Downie, C., 1979. A stratified water column environmental model for the type Kimmeridge Clay. Nature 277, 377–380.

van Dongen, B.E., Schouten, S., Sinninghe Damstè, J.S., 2006. Preservation of carbohydrates through sulfurization in a Jurassic euxinic shelf sea. Examination of the Blackstone Band TOC cycle in the Kimmeridge Clay Formation, UK. Org. Geochem. 37, 1052–1073. http://dx.doi.org/10.1016/j.orggeochem.2006.05.007.

van Kaam-Peters, H.M.E., Schouten, S., Köster, J., Sinninghe Damstè, J.S., 1998. Controls on the molecular and carbon isotopic composition of organic matter deposited in a Kimmeridgian euxinic shelf sea: evidence for preservation of carbohydrates through sulfurisation. Geochim. Cosmochim. Acta 62, 3259–3283.

Vlahović, I., Tišljar, J., Velić, I., Matičec, D., 2005. Evolution of the Adriatic Carbonate Platform: palaeogeography, main events and depositional dynamics. Palaeogeogr. Palaeoclimatol. Palaeoecol. 220, 333–360. http://dx.doi.org/10.1016/j.palaeo.2005.01.011.

Widdowson, M., Walsh, J.N., Subbarao, K.V., 1997. The geochemistry of Indian bole horizons: palaeoenvironmental implications of Deccan intravolcanic palaeosurfaces. In: Widdowson, M. (Ed.), Palaeosurfaces: Recognition, Reconstruction and Palaeoenvironmental Interpretation. In: Geological Society of London Special Publication, vol. 120, pp. 269–281.

Wignall, P., 2001. Large igneous provinces and mass extinctions. Earth-Sci. Rev. 53, 1–33.

Wignall, P., 2005. The link between large igneous province eruptions and mass extinctions. Elements 1, 293–297. http://dx.doi.org/10.2113/gselements.1.5.293.

Wignall, P.B., Newton, R.J., Little, C.R., 2005. The timing of paleoenvironmental change and cause-and-effect relationships during the Early Jurassic mass extinction in Europe. Am. J. Sci. 305, 1014–1032. http://dx.doi.org/10.2475/ajs.305.10.1014.

Witt, M.L.I., Mather, T.A., Pyle, D.M., Aiuppa, A., Bagnato, E., Tsanev, V.I., 2008. Mercury and halogen emissions from Masaya and Telica volcanoes, Nicaragua. J. Geophys. Res., Solid Earth 113, B06203. http://dx.doi.org/10.1029/2007JB005401.

Zheng, X., Jenkyns, H.C., Gale, A.S., Ward, D.J., Henderson, G.M., 2013. Changing ocean circulation and hydrothermal inputs during Ocean Anoxic Event 2 (Cenomanian–Turonian): evidence from Nd-isotopes in the European shelf sea. Earth Planet. Sci. Lett. 375, 338–348. http://dx.doi.org/10.1016/j.epsl.2013.05.053.